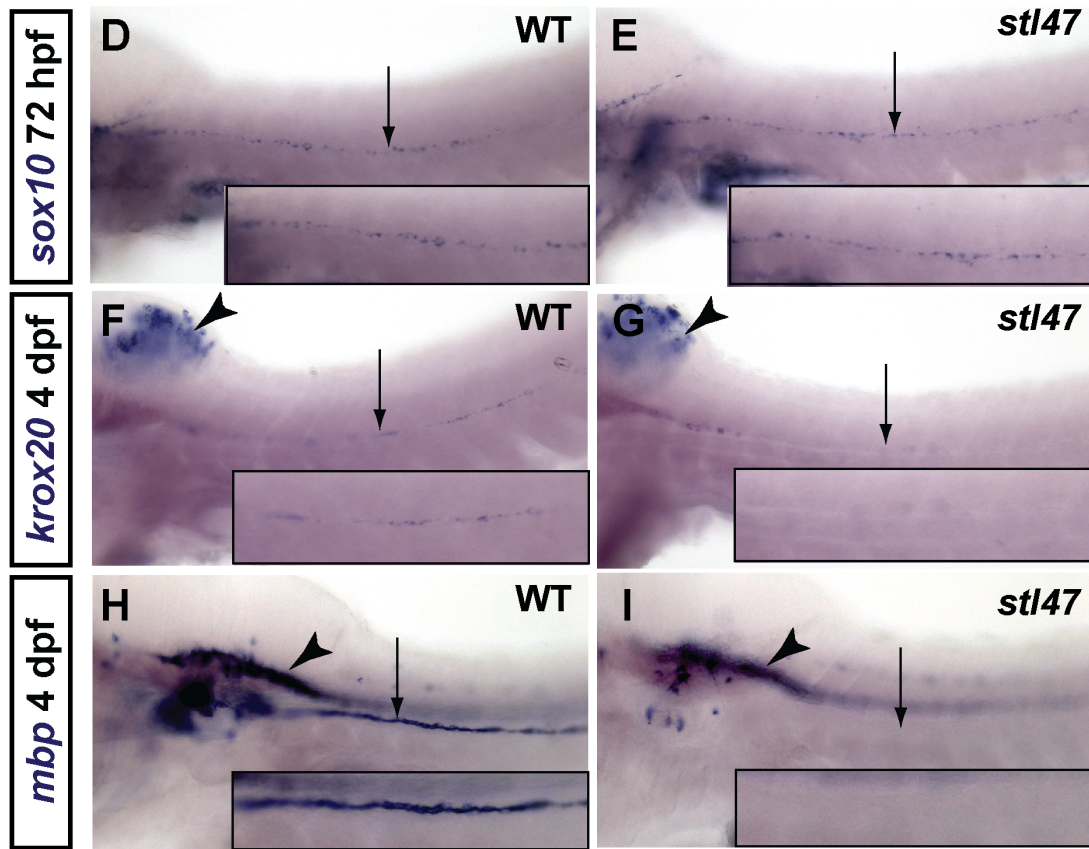
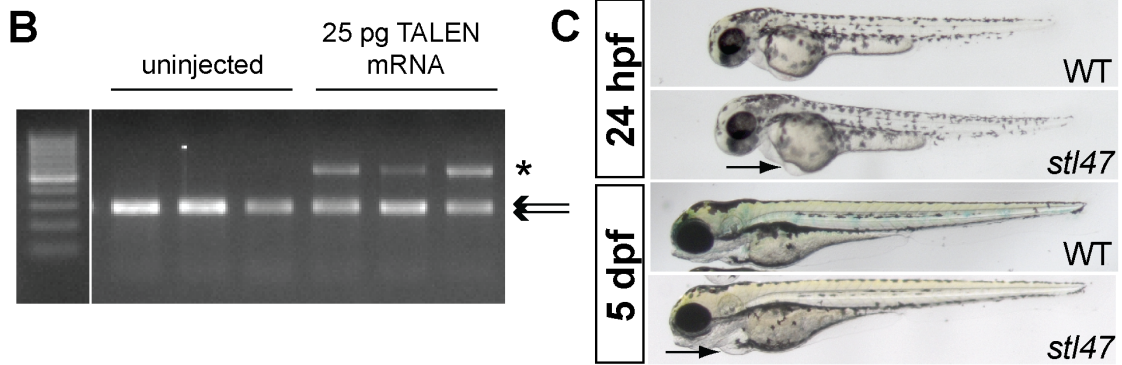


Figure S1

A left arm recognition sequence **MfeI** right arm recognition sequence
 ...TGACTACCCACCCAGCCAGTC CTG**CAATTG**GACCATA CAGGCCCCGGCTGGCTTTATA...



J

PLLn expression:	<i>sox10</i>		<i>krox20</i>		<i>mbp</i>	
	48 hpf	72 hpf	72hpf	4 dpf	4 dpf	4 dpf MZ
WT	26/26 (100%)	27/27 (100%)	16/16 (100%)	16/16 (100%)	34/34 (100%)	-
<i>gpr126^{stl47}</i>	9/9 (100%)	8/8 (100%)	0/8 (0%)	1/7 (14%)	6/14 (42%)	0/29 (0%)

Figure S2

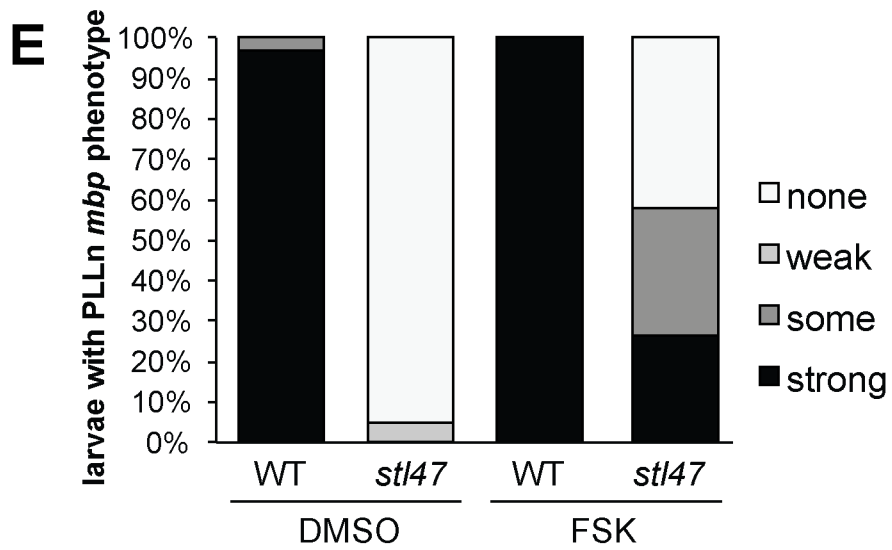
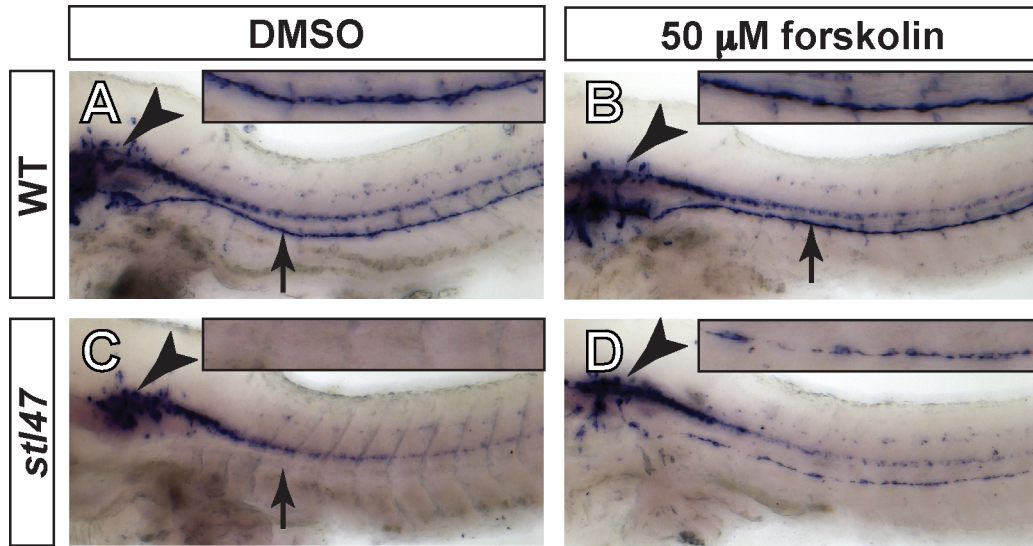


Figure S3

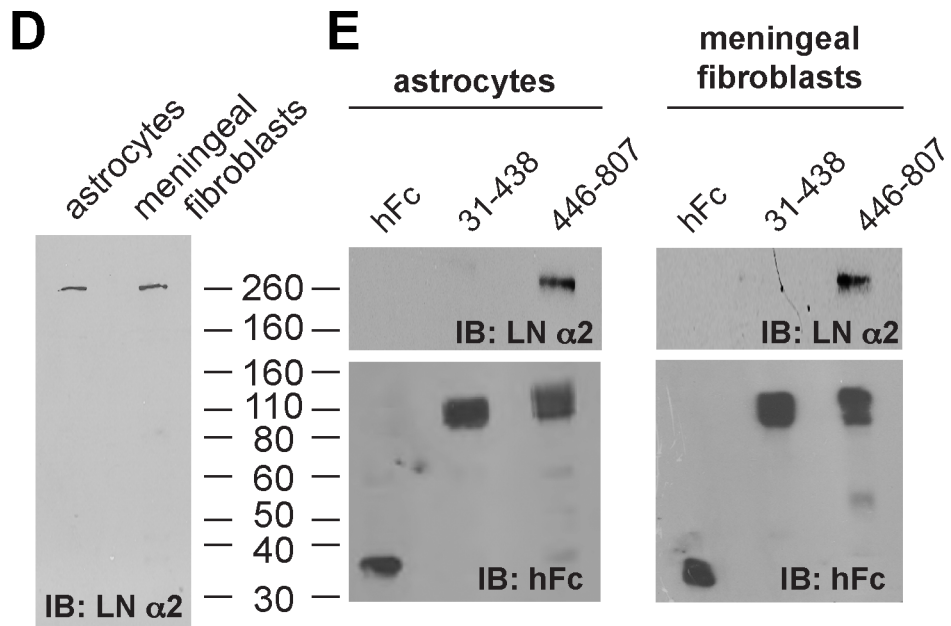
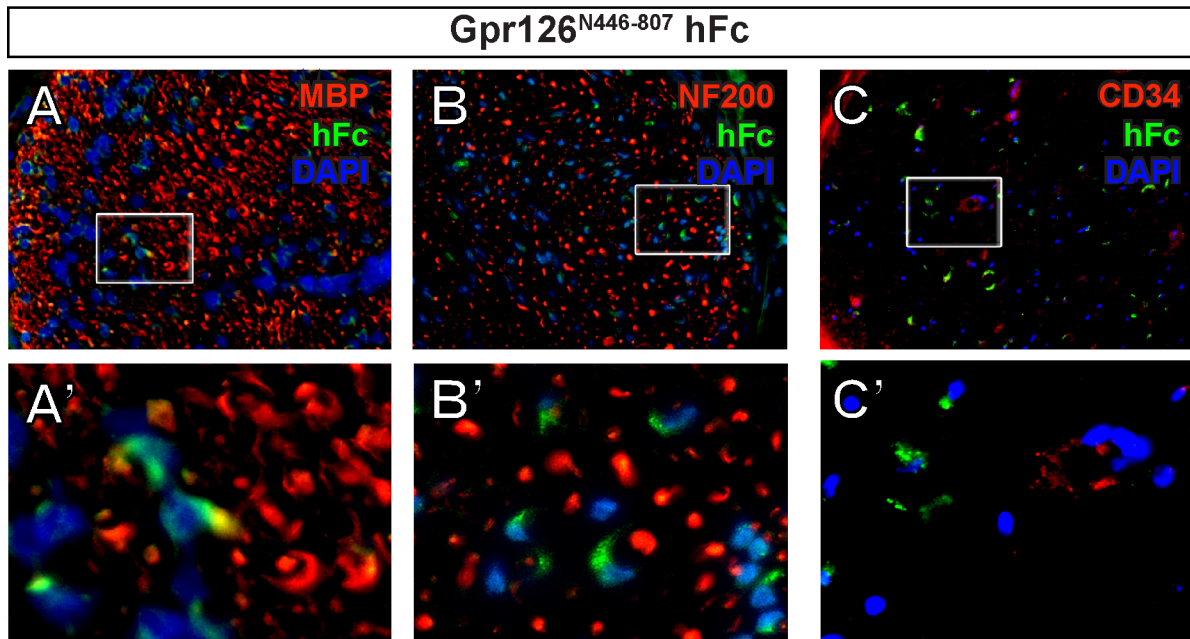


Figure S4

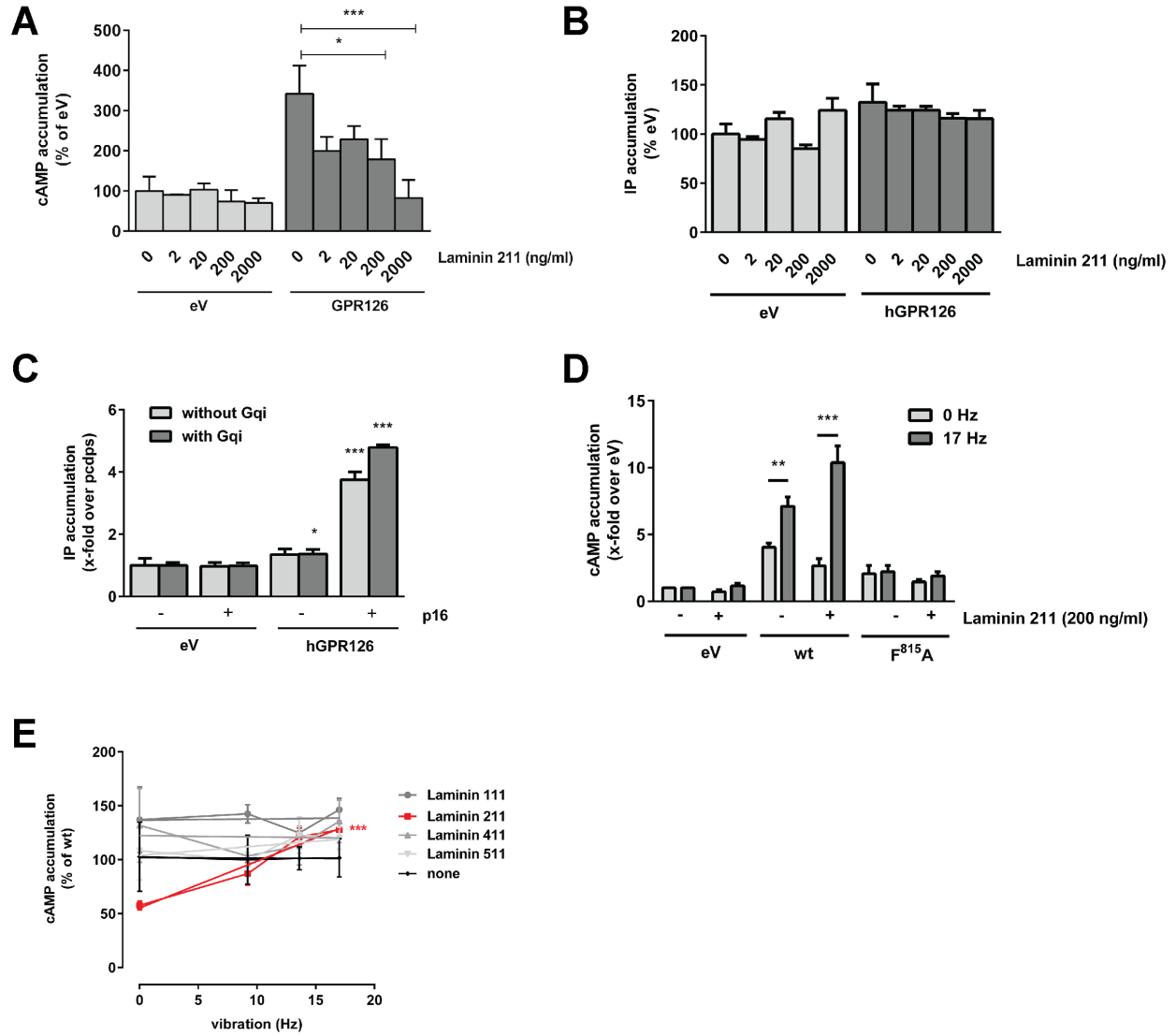


Figure S5

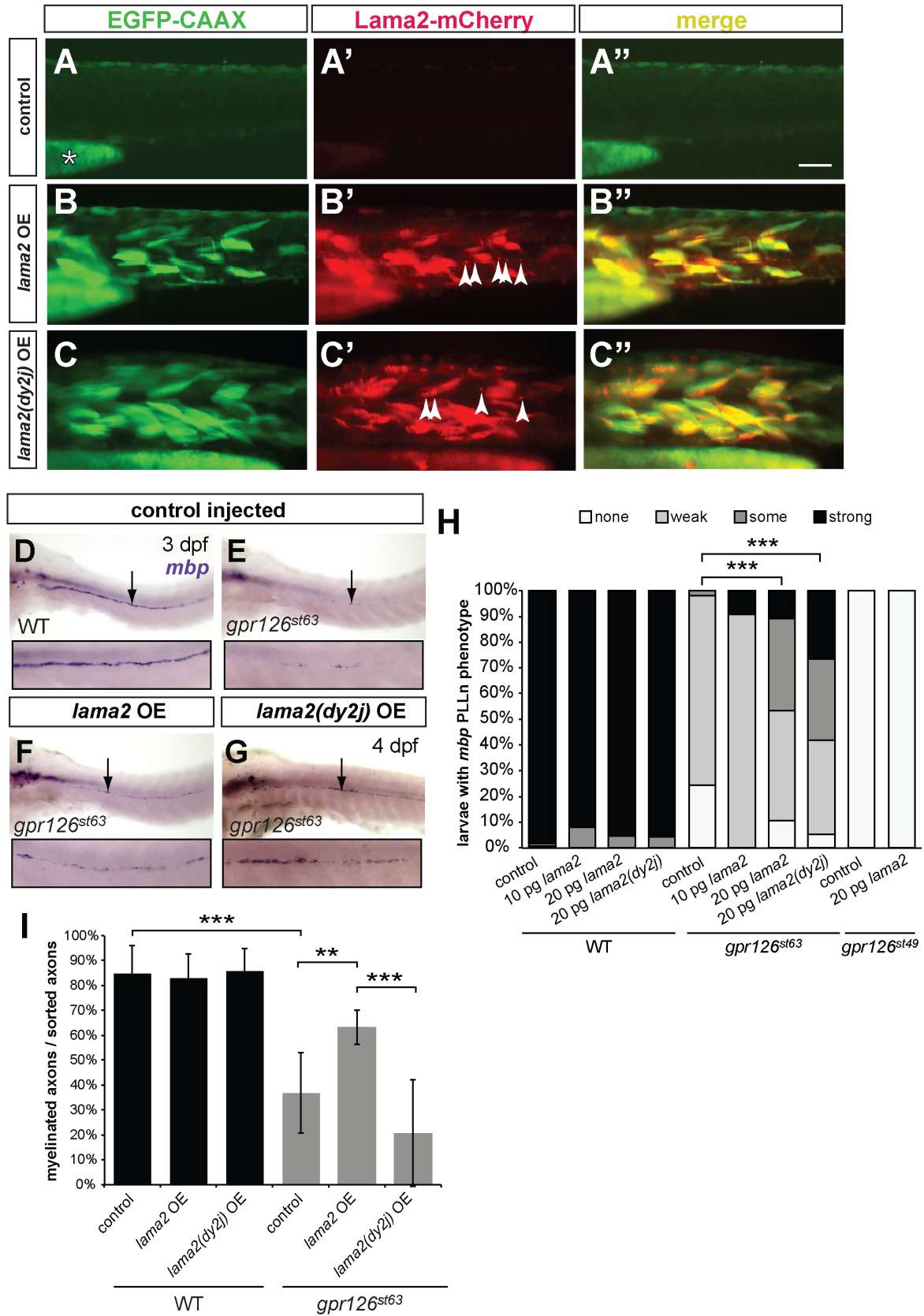


Figure S6

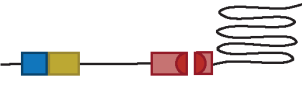



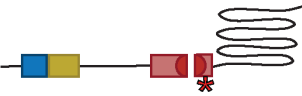


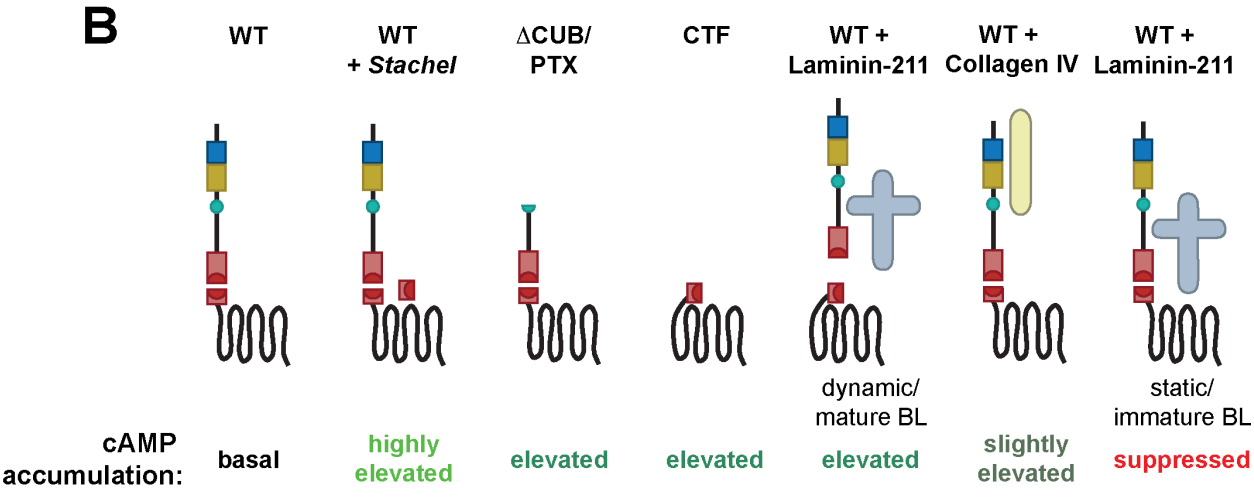
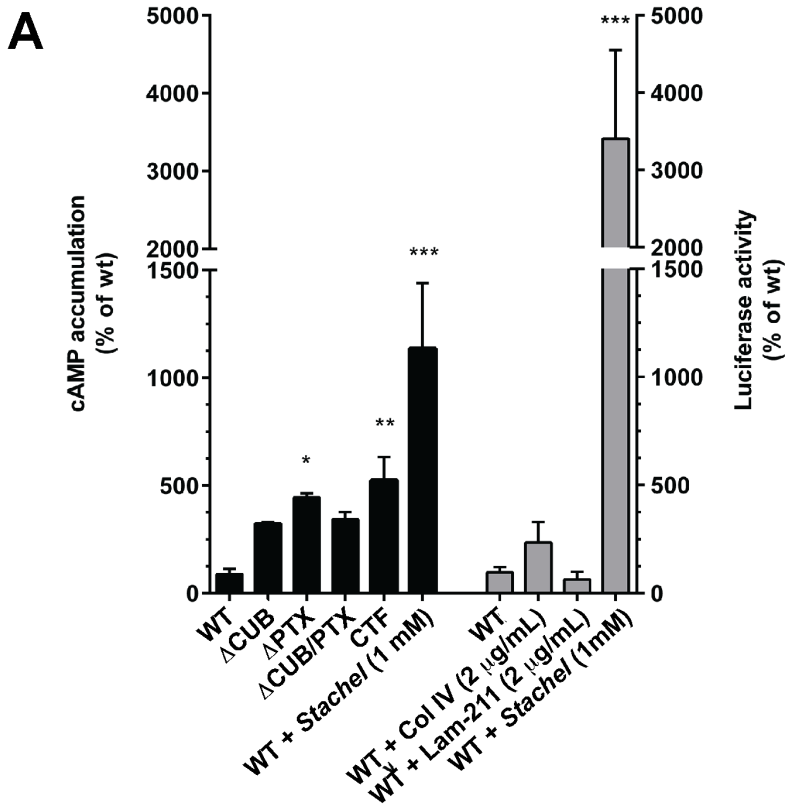
predicted Gpr126 structure	genotype	# sorted axons/ nerve	# myelinated axons/ nerve	# nerves analyzed	reference
3 dpf					
	WT	8 ± 1	6 ± 2	12	Figure 5
	WT + <i>lama2</i> MO	5 ± 2	3 ± 2	11	Figure 5
	<i>gpr126^{st63}</i>	6 ± 2	1 ± 1	5	Figure 5
	<i>gpr126^{st63}</i> + <i>lama2</i> MO	2 ± 1	0	6	Figure 5
5 dpf					
	WT	13 ± 1 12 ± 2	13 ± 1 10 ± 2	3 23	Monk <i>et al.</i> , 2009 Figures 1, 6
	<i>gpr126^{st49}</i> (zygotic)	11 ± 2	0	5	Monk <i>et al.</i> , 2009
	<i>gpr126^{st49}</i> (MZ)	8 ± 2	0	7	Figure 1
	<i>gpr126^{st49/st47}</i>	8 ± 2	0	9	Figure 1
	<i>gpr126^{sti215}</i> (zygotic <i>Stachel</i> mutant)	8 ± 2	0	6	Liebscher <i>et al.</i> , 2014
	<i>gpr126^{sti47}</i> (zygotic)	5 ± 2	0.5 ± 0.6	4	Figure 1
	<i>gpr126^{sti47}</i> (MZ)	1 ± 1	0	4	Figure 1
	<i>gpr126^{st63}</i> (zygotic)	9 ± 1	3 ± 1	7	Figure 6
	<i>gpr126^{st63}</i> + <i>lama2</i>	10 ± 2	7 ± 1	8	Figure 6
	<i>gpr126^{st63}</i> + <i>lama2(dy2j)</i>	7 ± 1	2 ± 2	7	Figure 6

Figure S7



SUPPLEMENTAL FIGURE LEGENDS

Figure S1, related to Figure 1. *gpr126*^{stl47} mutants fail to express markers of terminal Schwann cell (SC) differentiation. (A) TALEN-targeted sequence of *gpr126*. The endogenous MfeI site is indicated in red. (B) Restriction fragment length analysis of F0 embryo 24 hours post-fertilization (hpf) DNA. Three representative uninjected (WT) embryos have digestion of the PCR product by MfeI (arrows). Three representative embryos injected with TALEN mRNA (12.5 pg for each left and right TALEN arms) have mosaic disruption of the targeted *gpr126* locus indicated by undigested product (asterisk). (C) Gross morphology of WT and MZ *gpr126*^{stl47} zebrafish at 24 hpf and 5 dpf. Mutants are grossly normal with cardiac edema observed in some larvae (arrows). (D-I) Lateral views showing whole mount *in situ* hybridization (WISH) of zebrafish larvae. Location of the PLLn is marked with an arrow; staining in the central nervous system (CNS) is marked with an arrowhead. Inset panels show magnification of the PLLn. (D) *sox10* expression in the PLLn of WT and (E) *gpr126*^{stl47} larvae at 72 hpf. (F) *krox20* expression in the PLLn and CNS of WT larvae at 4 dpf. (G) *krox20* is expressed in the CNS but not the PLLn of *gpr126*^{stl47} mutants at 4 dpf. (H) *mbp* expression in the PLLn and CNS of WT larvae at 4dpf. (I) *mbp* is expressed in the CNS but not the PLLn of *gpr126*^{stl47} mutants at 4 dpf. (J) Quantification of WISH expressed as a percentage of larvae with PLLn expression out of total larvae scored. For all markers and timepoints, WT = *gpr126*^{+/+} and *gpr126*^{stl47/+} larvae. *gpr126*^{stl47} indicates zygotic mutants for all markers and timepoints except for *mbp* at 4dpf labeled MZ.

Figure S2, related to Figure 2. FSK rescues *mbp* expression in *gpr126*^{stl47} mutants.

(A-D) Lateral views of *mbp* expression via WISH of 5 dpf zebrafish larvae. PLLn is marked with arrows; CNS is marked with arrowheads. Inset panels show magnification of the PLLn. (A) *mbp* is strongly expressed in both DMSO-treated and (B) FSK-treated WT siblings. (C) *mbp* expression is lost in the PLLn of a DMSO-treated *gpr126*^{stl47} mutant, but (D) FSK treatment results in *mbp* expression in the PLLn of a *gpr126*^{stl47} mutant. (E) Quantification of WISH expressed as percentage of larvae with PLLn *mbp* expression out of total larvae scored. Phenotypes assigned as described (Liebscher et al., 2014). For all markers and timepoints, WT = *gpr126*^{+/+} and *gpr126*^{stl47/+} larvae.

Figure S3, related to Figure 3. GPR126-NTF specifically binds a SC-derived ligand and Laminin α 2.

(A-C) GPR126^{N446-807} specifically binds SCs. Anti-hFc immunostaining is green and nuclear counterstain is DAPI (blue). Magnification of the boxed regions in A-C is indicated in A'-C'. (A) GPR126^{N446-807} immunostaining colocalizes with MBP-labeled Schwann cells (red), but not (B) NF200-labeled axons (red) or (C) CD34-labeled fibroblasts. (D) Western blot showing abundant Laminin α 2 protein (LN α 2) produced by primarily cultured mouse astrocytes and meningeal fibroblasts. (E) GPR126^{N446-807} specifically binds Laminin α 2. Mouse primary meningeal fibroblasts or astrocytes were used as Laminin sources. Immunocomplexes were subjected to SDS-PAGE and western blot using mouse anti-Laminin α 2 antibody. Only GPR126^{N446-807} binds Laminin α 2.

Figure S4, related to Figure 6A-B. Laminin-211 specifically activates GPR126 via the *Stachel* sequence, and Laminin-211-mediated cAMP suppression in GPR126 is not mediated through G_i activation. (A) COS-7 cells were transiently transfected with empty vector (eV) and hGPR126 plasmid. cAMP accumulation was measured after stimulation with increasing concentrations of Laminin-211. Results are given as means \pm SEM of three independent assays each performed in triplicate. Statistics were performed by applying a two-way ANOVA in combination with Bonferroni as post-hoc test: * $p < 0.05$; ** $p < 0.01$; *** $p < 0.001$ (B) COS-7 cells were transfected with 500 ng of empty vector and WT hGPR126 constructs with the addition of the $G\alpha_{q/i}$ -chimera. Basal IP levels were determined as described in the methods section. Addition of increasing concentrations of Laminin-211 does not increase IP levels. Empty vector served as negative control (pcDps + G_{qi} : level: 100.0 ± 14.76 cpm). Data are given as means \pm SEM of one representative experiment performed in triplicates. (C) COS-7 cells were transfected with 500 ng of empty vector and WT hGPR126 constructs with or without the addition of the $G\alpha_{q/i}$ -chimera. Application of the *Stachel* sequence peptide (Liebscher et al., 2014) stimulated G_i and G_q pathway of GPR126. Empty vector served as negative control (pcDps: IP level: 51.0 ± 9.2 cpm; pcDps + G_{qi} : level: 76.0 ± 5.7 cpm). Data are given as means \pm SEM of one representative experiment performed in triplicates. (D) COS-7 cells were transfected with empty vector (eV), WT hGPR126 and the hGPR126 F⁸¹⁵A, respectively. cAMP accumulation was measured under static (0 Hz) and dynamic (17 Hz) conditions with and without Laminin-211. Vibration-induced cAMP induction is abolished in the GPR126 F⁸¹⁵ mutant that disrupts the tethered peptide agonist. Data is represented as mean \pm SEM of three independent assays each

performed in triplicate. Statistics were performed by applying a two-way ANOVA in combination with Sidak's multiple comparison test: * $p < 0.05$; ** $p < 0.01$; *** $p < 0.001$. (E) COS-7 cells were transiently transfected with empty vector (eV) and hGPR126 plasmid and cAMP accumulation was measured after stimulation with Laminins -111, -211, -411, and -511 under increasing vibration. Only Laminin-211 causes a significant frequency-dependent increase of cAMP accumulation, reversing the suppression observed under static conditions. Data is represented as mean \pm SEM of three independent assays each performed in triplicate. Statistics were performed analyzing linear regression for each curve: * $p < 0.05$; ** $p < 0.01$; *** $p < 0.001$

Figure S5, related to Figure 6C-K. Lama2 overexpression rescues *gpr126*^{st63} hypomorphic mutant *mbp* expression. (A-C'') Lateral views of mosaic transgenic expression of EGFP-CAAX and Lama2-mCherry (wild-type or *dy2j*) expression in 3 dpf larvae. Scale bar = 100 μ m. (A) Phenol red-injected sibling. No expression of EGFP or mCherry is observed. Asterisk indicates autofluorescence of the yolk extension in the green channel. (B) *acta1:lama2-mCherry:T2:EGFP-CAAX* injected larva. EGFP-CAAX labels mosaic expression of the construct in membranes of muscle cells. Lama2-mCherry (B') transgenic protein (arrowheads) is secreted near the region typically occupied by the PLLn. Note that these puncta do not overlap with the transgene-expressing muscle (B''). (C) *acta1:lama2(dy2j)-mCherry:T2:EGFP-CAAX* injected larva. Note expression of mutant *lama2(dy2j)* construct (green muscle fibers) and secretion of mCherry-tagged protein (arrowheads) is comparable to that of wild-type Lama2-mCherry. (D-G) Lateral views showing WISH of *mbp* expression in 3-4 dpf larvae.

Arrows indicate location of PLLn; magnification of PLLn is shown for each panel. (D) WT phenol red-injected *gpr126*^{+/+} sibling with strong *mbp* expression in PLLn. (E) Phenol red-injected *gpr126*^{st63/st63} hypomorphic mutant with very reduced *mbp* expression in PLLn. (F) Injection of *acta1:lama2-mCherry:T2:EGFP-CAAX* or (G) *acta1:lama2(dy2j)-mCherry:T2:EGFP-CAAX* into *gpr126*^{st63} mutants results in increased *mbp* in PLLn. (H) Quantification of WISH at 3-4 dpf expressed as a percentage of larvae with each *mbp* PLLn phenotype. “WT” = pooled *gpr126*^{+/+}, *gpr126*^{+/st63}, and *gpr126*^{+/st49} siblings. “Control” = pooled uninjected and phenol red-injected. *** p<0.001, Fisher’s exact test comparing “typical” *gpr126*^{st63/st63} phenotypes (“none” and “weak”) to “atypical” phenotypes (“some” and “strong”). (I) Percentage of myelinated axons among sorted axons from data shown in Figure 6I-J. ** p<0.01, *** p<0.001, Student’s t-test.

Figure S6, related to Figures 1, 5-6. Radial sorting and myelination phenotypes in zebrafish *gpr126* allelic series. Summary of radial sorting and myelination phenotypes obtained in ultrastructural analyses of 3 and 5 dpf zebrafish larvae in *gpr126* allelic series, including *lama2* knockdown and *lama2* rescue. “WT” for the present study includes pooled sibling data from *gpr126*^{stl47/+} and *gpr126*^{st63/+} in-crosses; “WT” for the Monk *et al.*, 2009 study includes sibling data from *gpr126*^{st49/+} in-crosses. Red asterisk in protein schematic indicates Cys>Tyr in *gpr126*^{st63} mutant and Δ6 *Stachel* deletion in *gpr126*^{stl215} mutant (Liebscher *et al.*, 2014).

Figure S7, related to Figures 6A-B, 7. Comparison of GPR126 activation. (A) COS-7 cells were transfected with empty vector, WT and mutant hGPR126 constructs that

lack either the indicated N-terminal domains or the complete N-terminal fragment. Basal cAMP levels or *Stachel* peptide stimulated cAMP levels were measured and displayed as percent of WT GPR126 activity level. Because Collagen IV-induced activation of the hGPR126 G_s pathway could not be detected in classic cAMP experiments, a comparable approach was used to measure Laminin-211, Collagen type IV, and *Stachel* peptide induced response using the more sensitive CREB-luciferase reporter gene assay. Here, empty vector, WT and mutant hGPR126 constructs were co-transfected with CREB-luciferase reporter plasmid in HEK293T cells. Again, results are shown as percent of WT luciferase levels. It is conceivable that the hGPR126 Collagen IV-induced response is comparable with or even smaller than the activation increase observed upon deletion of the Collagen IV binding domain. Data is represented as mean ± SEM of three independent assays each performed in triplicate. Statistics were performed by applying a one-way ANOVA in combination with Bonferroni as post-hoc test: * p<0.05; ** p<0.01; *** p<0.001. **(B)** Schematic summary of cAMP accumulation in heterologous cells using various hGPR126 constructs, ECM molecules, and dynamic forces. Data summarized in schematic representation are taken from Figure 6A-B and panel A.

SUPPLEMENTAL METHODS

Animals

All animal experiments were performed in compliance with institutional animal protocols. The *Lama2^{dy3k}*, SC-specific *Gpr126*, and *Gpr126* mutants were described previously (Miyagoe et al., 1997; Mogha et al., 2013; Monk et al., 2011). For ligand binding and immunostaining experiments, WT mice on the CD-1 strain (Charles River Laboratories) were used. For P3 nerve co-IP experiments, WT mice on the C57/BL6N strain (Charles River Laboratories) were used. Adult zebrafish were maintained in the Washington University Zebrafish Consortium facility (<http://zebrafish.wustl.edu/husbandry.htm>). Embryos were collected from harem matings, raised at 28.5°C, and staged according to standard protocols (Kimmel et al., 1995). The following adult strains were generated and/or maintained for this paper: WT AB*, *gpr126^{st49}* (Monk et al., 2009; Pogoda et al., 2006), *gpr126^{st63}* (Monk et al., 2009; Pogoda et al., 2006), *gpr126^{stl47}*. Adult mutant strains were maintained as heterozygous stocks for zygotic mutant experiments with WT sibling controls (Figures 1, 2, 5, 6, S1, S2, S5, S6) and as homozygous mutant stocks for maternal-zygotic (MZ) experiments (Figures 1, S6).

Sample numbers for zebrafish TEM are as follows: for Figure 1, n = 11 WT nerves (3 *gpr126^{+/+}*, 8 *gpr126^{+/stl47}*) in 7 larvae, n = 7 *gpr126^{st49/st49}* MZ nerves in 4 larvae, n = 4 *gpr126^{stl47/stl47}* Z nerves in 3 larvae, n = 4 *gpr126^{stl47/stl47}* MZ nerves in 4 larvae, n = 9 *gpr126^{st49/stl47}* nerves in 5 larvae; for Figure 2, n = 6 DMSO-treated WT nerves (3 *gpr126^{+/+}*, 3 *gpr126^{stl47/+}*) in 4 larvae, n = 5 FSK-treated WT nerves (3 *gpr126^{+/+}*, 2 *gpr126^{+/stl47}*) in 3 larvae, n = 3 DMSO-treated *gpr126^{stl47/stl47}* nerves in 3

larvae, and n = 7 FSK-treated *gpr126*^{stl47/stl47} nerves in 4 larvae; for Figure 5, n = 12 uninjected WT nerves (6 *gpr126*^{+/+}, 6 *gpr126*^{+/st63}) in 7 larvae, n = 11 5 ng MO-injected WT nerves (5 *gpr126*^{+/+}, 6 *gpr126*^{+/st63}) in 7 larvae, n = 5 uninjected *gpr126*^{st63/st63} nerves in 3 larvae, and n = 6 5 ng MO-injected *gpr126*^{st63/st63} nerves in 3 larvae; for Figure 6, n = 12 uninjected WT nerves (6 *gpr126*^{+/+}, 6 *gpr126*^{+/st63}) in 7 larvae, n = 12 *lama2* OE WT nerves (8 *gpr126*^{+/+}, 4 *gpr126*^{+/st63}) in 7 larvae, n = 5 *lama2(dy2j)* OE WT nerves (3 *gpr126*^{+/+}, 2 *gpr126*^{+/st63}) in 4 larvae, n = 7 uninjected *gpr126*^{st63/st63} nerves in 6 larvae, n = 8 *lama2* OE *gpr126*^{st63/st63} nerves in 5 larvae, and n = 7 *lama2(dy2j)* OE *gpr126*^{st63/st63} nerves in 4 larvae.

Sample numbers for zebrafish WISH are as follows: for Figure 5, N = 3 biological and 2 technical replicates, n = 150 control (36 *gpr126*^{+/+}, 75 *gpr126*^{+/st63}, 39 *gpr126*^{st63/st63}), 72 2.5 ng MO-injected (19 *gpr126*^{+/+}, 36 *gpr126*^{+/st63}, 17 *gpr126*^{st63/st63}), and 50 5 ng MO-injected (12 *gpr126*^{+/+}, 29 *gpr126*^{+/st63}, 9 *gpr126*^{st63/st63}); for Figure S2, N = 4 biological and 3 technical replicates, n = 84 WT (33 DMSO-treated, 51 FSK-treated) and n = 49 *gpr126*^{stl47} (20 DMSO-treated, 19 FSK-treated); Figure S5, N = 6 biological and 4 technical replicates, n = 230 WT (127 control, 37 10 pg *lama2*-injected, 43 20 pg *lama2*-injected, 43 20 pg *lama2(dy2j)*-injected), n = 111 *gpr126*^{st63/st63} (53 control, 11 10 pg *lama2*-injected, 28 20 pg *lama2*-injected, 19 20 pg *lama2(dy2j)*-injected), and n = 23 *gpr126*^{st49/st49} (10 control, 13 20 pg *lama2*-injected). Sample numbers for Figure S1 are reported within the figure.

Zebrafish genotyping

st49 and *st63* were genotyped as previously described (Monk et al., 2009). For *stl47*, the following primer pair was used to amplify a 498-base pair (bp) product from genomic DNA: F: 5'-GTCTTTGTCTCTGTTCGATGC-3' and R: 5'-GCTTGTAAGTATGATGGAAGCC-3'. PCR product from WT DNA is cleaved by MfeI restriction digest to yield 257-bp and 241-bp fragments. The $\Delta 5+3$ indel in *stl47* disrupts the MfeI recognition site and the 498-bp product is retained.

Generation of *stl47* mutants

Left and right TALEN constructs in the pCS2+ backbone were designed using the TALEN targeter tool (<https://tale-nt.cac.cornell.edu/>) and generated using the GoldyTALEN kit previously described (Bedell et al., 2012). Left repeat variable diresidue (RVD) sequence: NN NI HD NG NI HD HD HD NI HD HD HD NI NN HD HD NI NN NG HD. Right RVD sequence: NI NG NI NI NI NN HD HD NI NN HD HD NN NN NN NN HD HD NG NN. Transcription of TALEN mRNA from pCS2+ constructs was separately performed with the mMESSAGING mMACHINE® SP6 ULTRA kit (Ambion). Left and right mRNAs were then combined in equimolar amounts (25 pg/nL total) and microinjected into 1-cell stage AB* embryos. Germline founders for F0 *gpr126* mutants were identified by raising F0s to adulthood and crossing to WT AB adults. Genomic DNA was extracted from 24 hpf progeny of these matings and genotyped as described above. The *stl47* lesion (and others) was identified by cloning the amplicon described above into pCRII via TOPO® TA Cloning® kit (Invitrogen) and Sanger sequencing the product.

Zebrafish immunostaining, whole-mount *in situ* hybridization (ISH), and analysis

For WISH, larvae were raised in egg water + 0.003% PTU and fixed with 4% paraformaldehyde at 3 or 4 dpf stage (Kimmel et al., 1995). WISH was performed using standard protocols (Thisse et al., 1994). The following established riboprobes were used for this study: *sox10*, *krox20* (Pogoda et al., 2006) and *mbp* (Lyons et al., 2005). PLLn expression was scored with observer blind to genotype and treatment. For p-FAK immunostaining, transgenic *sox10:mRFP* were raised in egg water to 4 dpf and fixed in 4% paraformaldehyde. Immunostaining was performed as previously described (Bae et al., 2009) with rabbit anti-phosphorylated FAK monoclonal antibodies from Invitrogen (catalog #44-625G). With the exception of MZ experiments, all experiments were performed with an in-cross of heterozygous parents for comparison to WT siblings. Expression scoring was performed with observer blind to genotype and treatment according to the following rubric (Liebscher et al., 2014): “strong” = strong and consistent expression throughout PLLn, “some” = weak but consistent expression in PLLn, “weak” = weak and patchy expression in PLLn, “none” = no expression in PLLn.

Zebrafish transmission electron microscopy (TEM) and analysis

Larvae were raised to 3 or 5 dpf (Kimmel et al., 1995) and processed for TEM as previously described (Czopka and Lyons, 2011) using a Pelco BioWave Pro with Steady Temp Plus water recirculation system (Ted Pella Inc.). Ultrathin sections were mounted on mesh copper grids and stained with saturated uranyl acetate and Sato’s lead stain. Samples were viewed with a Jeol JEM-1400 (Jeol USA) and micrographs were obtained with an AMT V601 digital camera (Advanced Microscopy Techniques Corp). To avoid

developmental differences along the anterior-posterior axis, larvae were analyzed between segments 5-6 at 3 dpf and segments 5-7 at 5 dpf. Analysis of axon number, number of sorted axons, and number of myelinated axons per nerve was performed with ImageJ software with observer blind to genotype and/or treatment. The developing zebrafish PLLn differs in its geometry compared to developing mammalian nerves in that endoneurial space is not evident and distinct SC compartments are not as readily observed in zebrafish larvae as in mammals. Axons were scored as sorted if, in the field of view examined: 1) they were fully ensheathed by 1-1.5 turns of SC cytoplasm; 2) the ensheathing SC could be clearly delineated from neighboring SCs by cytoplasmic boundaries; 3) the ensheathing SC did not sort any other axon. These parameters have been previously employed to assess sorting of axons by SCs in zebrafish (e.g., Monk et al., 2009). Statistics were performed using 1-way ANOVA and Bonferroni's Multiple Comparisons Test with GraphPad Prism.

NTF plasmid constructions

Three different mouse GPR126-NTF constructs were built into the pFUSE-hFc2 vector (Invitrogen) that contains the IL2 signal peptide sequence and the human IgG Fc tag. The signal peptide of GPR126 is within aa 1-30. Full length GPR126-NTF (aa 31-807) and two shorter fragments (aa 31-438 and aa 446-807) were generated by PCR and subsequently fused to hFc to generate three human IgG Fc-tagged GPR126-NTFs, GPR126-NTF³¹⁻⁸⁰⁷-hFc, GPR126-NTF³¹⁻⁴³⁸-hFc, and GPR126-NTF⁴⁴⁶⁻⁸⁰⁷-hFc. The PCR primers for mouse GPR126-NTF are as follows: Forward Primer 31: 5'-

CACGAATTCGGTTCCTCTCTCAGTGTGCGG-3'; Reverse Primer 807: 5'-
GTTAGATCTGCACAGACAAATGGTCTCACC-3'

Reverse Primer 438: 5'-GTTAGATCTGATTTTCATCCTGTCCTCTCC-3'

Forward Primer 446F: 5'-CACGAATTCGGACAAAAGGTTGGTGCTCTGC-3'

Generation of hFc fusion protein

Each of the above GPR126-NTF-hFc expression constructs was transiently transfected into HEK-293T cells. 24 hours after transfection, the culture media was changed to serum-reduced OPTI-MEM media. The conditioned media was harvested 48-72 hours later, followed by concentration and column purification, as previously described (Luo et al., 2011).

Putative ligand binding assay

Putative ligand binding *in situ* was performed on fresh frozen nerves, as previously described (Luo et al., 2011). Briefly, 12 µm thick sections were on a cryostat (Leica). Equivalent amounts of fusion proteins were used as probes to examine their binding ability to mouse sciatic nerve sections. The localizations of GPR126-hFc proteins were visualized by fluorescein-conjugated rabbit anti-human IgG antibody (Thermo Scientific).

Co-immunoprecipitation (co-IP), western blot analysis, and immunohistochemistry (IHC)

Co-IP and immunoblotting were performed as previously described (Luo et al., 2011). Astrocytes and meningeal fibroblasts produce abundant Laminin-211, and therefore were used as a ligand source. Mouse primary astrocytes were isolated from P1 mouse brains and cultured as mixed glia culture for 10 days in DMEM with 10% fetal bovine serum (FBS). Other glial cells (oligodendrocytes and microglia) were removed through shaking at 250 rpm overnight (O'Meara et al., 2011). Mouse primary meningeal fibroblasts were established from the meninges of E14.5 mice, and amplified in DMEM with 10% FBS (Luo et al., 2011). Protein-G beads were used to pull-down the GPR126-NTF-hFc protein complex. Immunocomplexes were subjected to SDS-PAGE and western blot using mouse anti-Laminin alpha2 antibody (Santa Cruz, SC-55605), and rabbit anti-human IgG Fc antibody (Thermo Scientific) following standard protocols. Immunohistochemistry was performed as previously described (Jeong et al., 2012) using the following antibodies: mouse monoclonal anti-S-100 (β -Subunit) (Sigma, S2532), rabbit polyclonal anti-s100 (Dako, z0311; Figure 3G and S3), rat anti-MBP (AbD Serotec), rat anti-CD34 (eBioscience, 14-0341-81), mouse anti-NF200 (Sigma, N0142) and appropriate secondary antibodies (Life Technologies and Molecular Probes). The C-terminal peptide of mouse GPR126 (CTSKSKSSSTTYFKRNSHSDNFS) was used to immunize rabbits for antiserum production (Yenzym Antibodies). For nerve co-IP, P3 sciatic nerves were powdered and resuspended in ice-cold RIPA buffer (50 mM Tris pH 7.4, 150 mM NaCl, 1% Nonidet P-40, SDS 0.1%, 1 mM EDTA) with protease inhibitor cocktail (Sigma Aldrich, St. Louis,

MO) and lysed under agitation at 4°C for 10 min. The lysates were cleared of insoluble materials by centrifugation at 13,000 x g for 10 min at 4°C. Protein concentration was determined by BCA protein assay method (Thermo Scientific, Waltham, MA) according to the manufacturer's protocol, and 250 µg protein was used for immunoprecipitation. Nerve lysates were pre-cleared with protein G sepharose beads (GE Healthcare) at 4°C for 1 h, followed by incubation with 2 µg of hFc or Gpr126-NTF-hFc fusion proteins for 3h and 1h with 40 µl of protein G sepharose beads. After extensive washes, the immunopurified proteins were denatured in 3X SDS sample buffer, separated by SDS-PAGE gel, and transferred to a PVDF membrane. The membranes were then probed with mouse monoclonal anti-Laminin α 2 antibody (2D9 gift from Hisae Hori) using standard western blot protocols.

Mouse Dorsal root ganglia (DRG) cultures

DRGs were isolated from WT and *Gpr126*^{-/-} mouse embryos at E13.5 and were cultured in 48 well plates as previously described (Mogha et al., 2013) with slight modifications as followed. 48 well plates were coated with Poly D-Lysine (100 µg/ml) overnight followed by coating with Laminin-211 (0.2 µg/ml and 5 µg/ml) for two hours at 37°C. N = 4 technical replicates.

Morpholino injections

Knockdown of *lama2* was performed with an established *lama2* translation-blocking morpholino (MO) (Pollard et al., 2006) obtained from Gene Tools. Embryos were collected from *gpr126*^{st63/+} in-crosses and microinjected at the 1-cell stage with 1x

phenol red dye alone, 2.5 ng MO + 1x phenol red dye, or 5 ng MO + 1x phenol red dye. Larvae from any group with gross morphological defects were discarded prior to WISH or TEM. No differences were observed between phenol red dye-injected and uninjected larvae; these samples were therefore pooled as “control”.

***lama2(dy2j)* plasmid construction and Lama2-mCherry overexpression**

The *acta1:lama2-mCherry:T2:EGFP-CAAX* is an established Lama2-mCherry rescue/overexpression (OE) construct kindly provided by Peter Currie (Sztal et al., 2012). To produce *lama2(dy2j)*, 165 bp in this zebrafish cDNA construct were identified as homologous to the deletion in Domain IV likely produced in the M5 splice variant of *lama2(dy2j)* mice (Colognato et al., 1997; Xu et al., 1994). Briefly, a series of overlapping PCR using the *lama2* OE plasmid as template was performed between endogenous restriction enzymes sites (5' PacI, 3' BsiWI) in the *lama2* OE construct to generate a Δ 165 bp fragment. This deletion-containing fragment was then digested and ligated into the original *lama2* OE plasmid to generate a *lama2(dy2j)* OE construct. Precise excision of 165 bp and re-ligation of the fragment was confirmed via Sanger sequencing to ensure no additional mutations were introduced. The *lama2* and *lama2(dy2j)* OE DNA plasmids were each co-injected with Tol2 transposase mRNA (Asakawa et al., 2008) generated with the mMMESSAGE mMACHINE® SP6 ULTRA kit (Ambion). The following doses were injected: 10 pg DNA + 25 pg mRNA, 20 pg DNA + 25-50 pg mRNA. Proper expression and secretion of both wild-type and *dy2j* Lama2 protein from muscle was visually confirmed by virtue of the C-terminal mCherry fusion. Larvae with gross morphological defects or low/no transgenic expression (<4 transgenic

muscle fibers in PLLn region) were discarded prior to *in situ* hybridization or TEM fixation.

Generation of WT and mutant GPR126 constructs for heterologous expression

Full-length hGPR126 sequence, N- and C-terminally tagged, was inserted into the mammalian expression vector pcDps (Mogha et al., 2013). The point mutation F⁸¹⁵A was generated by PCR and homologous recombination in *E. coli* (Liebscher et al., 2014).

***In vitro* functional assays**

GPR126 constructs were heterologously expressed in COS-7 cells grown in Dulbecco's minimum essential medium (DMEM) supplemented with 10% FBS, 100 U/ml penicillin and 100 µg/ml streptomycin at 37°C and 5% CO₂ in a humidified atmosphere.

For cAMP accumulation assays, cells were split into 48-well plates (3×10⁴ cells/well) and transfected with 100 ng of plasmid using LipofectamineTM 2000 (Invitrogen) according to the manufacturer's protocol. Empty vector stimulated with 10 µM of forskolin served as positive controls. 48 h after transfection, cells were incubated with 3-isobutyl-methyl-xanthine (IBMX) (1 mM)-containing medium, lysed in LI buffer (PerkinElmer Life Sciences) and kept frozen at -20°C until measurement. To measure cAMP concentration, the AlphaScreen cAMP assay kit (PerkinElmer Life Sciences) was used as described (Mogha et al., 2013). Vibration was applied during incubation using a Heidolph Titramax 100 at 450 rpm; 1050 rpm and 1350 rpm resulting in a vibration of the incubator shelf at a frequency of 9.2 Hz, 13.6 Hz, and 17 Hz, respectively. For

shaking assays, COS-7 cells were seeded in 6 well plates (3×10^6 cells/well) and transfected with 1 μ g of plasmid DNA using LipofectamineTM 2000 (Invitrogen, Paisley, UK) according to the manufacturer's protocol. 48 h after transfection cells were harvested in 400 μ l Medium containing IBMX with and without the addition of Laminin-211 (BioLamina AB, Sundbyberg, Sweden). The cell/medium mix was incubated for 1 h at 37 °C standing or shaking at 50 or 100 rpm (Edmund Bühler GmbH; SH30;TH30), respectively. The assay was determined by centrifugation of the soluble cell mix (200 rpm, 2 min) and uptake into LI buffer (PerkinElmer Life Sciences) and kept frozen at -20°C until measurement. To measure cAMP concentration, the AlphaScreen cAMP assay kit (PerkinElmer Life Sciences) was used as described above.

IP accumulation assays were performed as described (Mogha et al., 2013). Briefly, cells were split into 12-well plates and transfected with 500 ng of plasmid DNA using LipofectamineTM 2000 (Invitrogen, Paisley, UK) according to the manufacturer's protocol. To measure IP formation, transfected COS-7 cells were incubated with 2 μ Ci/ml myo-[³H]inositol (18.6 Ci/mmol, PerkinElmer Life Sciences) for 16 h. Thereafter, cells were washed once with serum-free DMEM containing 10 mM LiCl followed by incubation with serum-free DMEM containing 10 mM LiCl. Intracellular IP levels were determined by anion-exchange chromatography as described (Berridge, 1983).

CREB-luciferase reporter gene assay was performed as described (Bohnekamp and Schoneberg, 2011). Specifically, HEK293T cells were grown in DMEM supplemented with 10% fetal bovine serum, 100 units/ml penicillin, and 100 μ g/ml streptomycin at 37 °C in a humidified 5% CO₂ incubator. One day prior to transfection, cells were split into

96-well cell culture plates (3.0×10^4 cells/well), and 24 h later, cells were co-transfected with the eV and GPR126 expression plasmid (20ng/well each) and the CREB-Luciferase reporter plasmid (50 ng/well; PathDetect CREB trans-reporting System). LipofectamineTM 2000 (Invitrogen) was used for transient transfection. After transfection, cells were maintained in antibiotic-free medium (serum 10%) throughout the experiments. One day after transfection, cells were treated with Laminin (Biolamina) or human Collagen type IV (C5533, Sigma-Aldrich, Taufkirchen, Germany), respectively in an assay volume of 100 μ l medium for 5 h. The assay was terminated by washing the cells twice with PBS and addition of 100 μ l luciferase assay reagent (SteadyLite, Perkin Elmer LAS, Rodgau-Jügesheim, Germany) and fluorescence was measured with a Victor 2 1420 Multilabel counter (PerkinElmer LAS, Rodgau-Jügesheim, Germany). Second messenger and reporter gene assay data were analyzed using GraphPad Prism version 6.0 for Windows (GraphPad Software).

SUPPLEMENTAL REFERENCES

- Asakawa, K., Suster, M.L., Mizusawa, K., Nagayoshi, S., Kotani, T., Urasaki, A., Kishimoto, Y., Hibi, M., and Kawakami, K. (2008). Genetic dissection of neural circuits by Tol2 transposon-mediated Gal4 gene and enhancer trapping in zebrafish. *Proc Natl Acad Sci U S A* *105*, 1255-1260.
- Bae, Y.K., Kani, S., Shimizu, T., Tanabe, K., Nojima, H., Kimura, Y., Higashijima, S., and Hibi, M. (2009). Anatomy of zebrafish cerebellum and screen for mutations affecting its development. *Developmental biology* *330*, 406-426.
- Bedell, V.M., Wang, Y., Campbell, J.M., Poshusta, T.L., Starker, C.G., Krug Ii, R.G., Tan, W., Penheiter, S.G., Ma, A.C., Leung, A.Y., *et al.* (2012). In vivo genome editing using a high-efficiency TALEN system. *Nature*.
- Berridge, M.J. (1983). Rapid accumulation of inositol trisphosphate reveals that agonists hydrolyse polyphosphoinositides instead of phosphatidylinositol. *Biochem J* *212*, 849-858.
- Bohnekamp, J., and Schoneberg, T. (2011). Cell adhesion receptor GPR133 couples to Gs protein. *J Biol Chem* *286*, 41912-41916.
- Colognato, H., MacCarrick, M., O'Rear, J.J., and Yurchenco, P.D. (1997). The laminin alpha2-chain short arm mediates cell adhesion through both the alpha1beta1 and alpha2beta1 integrins. *J Biol Chem* *272*, 29330-29336.
- Czopka, T., and Lyons, D.A. (2011). Dissecting mechanisms of myelinated axon formation using zebrafish. *Methods Cell Biol* *105*, 25-62.
- Jeong, S.J., Luo, R., Li, S., Strokes, N., and Piao, X. (2012). Characterization of G protein-coupled receptor 56 protein expression in the mouse developing neocortex. *J Comp Neurol* *520*, 2930-2940.
- Kimmel, C.B., Ballard, W.W., Kimmel, S.R., Ullmann, B., and Schilling, T.F. (1995). Stages of embryonic development of the zebrafish. *Dev Dyn* *203*, 253-310.
- Liebscher, I., Schön, J., Petersen, S.C., Fischer, L., Auerbach, N., Demberg, L.M., Mogha, A., Cöster, M., Simon, K.-U., Rothmund, S., *et al.* (2014). A tethered agonist within the ectodomain activates the adhesion G protein-coupled receptors GPR126 and GPR133. *Cell Rep*, in press.
- Luo, R., Jeong, S.J., Jin, Z., Strokes, N., Li, S., and Piao, X. (2011). G protein-coupled receptor 56 and collagen III, a receptor-ligand pair, regulates cortical development and lamination. *Proc Natl Acad Sci U S A* *108*, 12925-12930.
- Lyons, D.A., Pogoda, H.M., Voas, M.G., Woods, I.G., Diamond, B., Nix, R., Arana, N., Jacobs, J., and Talbot, W.S. (2005). *erbb3* and *erbb2* are essential for schwann cell migration and myelination in zebrafish. *Curr Biol* *15*, 513-524.
- Miyagoe, Y., Hanaoka, K., Nonaka, I., Hayasaka, M., Nabeshima, Y., Arahata, K., and Takeda, S. (1997). Laminin alpha2 chain-null mutant mice by targeted disruption of the *Lama2* gene: a new model of merosin (laminin 2)-deficient congenital muscular dystrophy. *FEBS Lett* *415*, 33-39.
- Mogha, A., Benesh, A.E., Patra, C., Engel, F.B., Schoneberg, T., Liebscher, I., and Monk, K.R. (2013). *Gpr126* functions in Schwann cells to control differentiation and myelination via G-protein activation. *J Neurosci* *33*, 17976-17985.

Monk, K.R., Naylor, S.G., Glenn, T.D., Mercurio, S., Perlin, J.R., Dominguez, C., Moens, C.B., and Talbot, W.S. (2009). A G protein-coupled receptor is essential for Schwann cells to initiate myelination. *Science* 325, 1402-1405.

Monk, K.R., Oshima, K., Jors, S., Heller, S., and Talbot, W.S. (2011). Gpr126 is essential for peripheral nerve development and myelination in mammals. *Development* 138, 2673-2680.

O'Meara, R.W., Ryan, S.D., Colognato, H., and Kothary, R. (2011). Derivation of enriched oligodendrocyte cultures and oligodendrocyte/neuron myelinating co-cultures from post-natal murine tissues. *J Vis Exp*.

Pogoda, H.M., Sternheim, N., Lyons, D.A., Diamond, B., Hawkins, T.A., Woods, I.G., Bhatt, D.H., Franzini-Armstrong, C., Dominguez, C., Arana, N., *et al.* (2006). A genetic screen identifies genes essential for development of myelinated axons in zebrafish. *Dev Biol* 298, 118-131.

Pollard, S.M., Parsons, M.J., Kamei, M., Kettleborough, R.N., Thomas, K.A., Pham, V.N., Bae, M.K., Scott, A., Weinstein, B.M., and Stemple, D.L. (2006). Essential and overlapping roles for laminin alpha chains in notochord and blood vessel formation. *Developmental biology* 289, 64-76.

Sztal, T.E., Sonntag, C., Hall, T.E., and Currie, P.D. (2012). Epistatic dissection of laminin-receptor interactions in dystrophic zebrafish muscle. *Hum Mol Genet* 21, 4718-4731.

Thisse, C., Thisse, B., Halpern, M.E., and Postlethwait, J.H. (1994). Goosecoid expression in neurectoderm and mesendoderm is disrupted in zebrafish cyclops gastrulas. *Developmental biology* 164, 420-429.

Xu, H., Wu, X.R., Wewer, U.M., and Engvall, E. (1994). Murine muscular dystrophy caused by a mutation in the laminin alpha 2 (Lama2) gene. *Nat Genet* 8, 297-302.